

Characterization of small (≤ 3 cm) hepatic lesions with atypical enhancement feature and hypointensity in hepatobiliary phase of gadoxetic acid-enhanced MRI in cirrhosis

A STARD-compliant article

Seung Kak Shin, MD^a, Yun Soo Kim, MD^{a,*}, Seung Joon Choi, MD^b, Young Sup Shim, MD^b, Dong Hae Jung, MD^c, Oh Sang Kwon, MD^a, Duck Joo Choi, MD^a, Ju Hyun Kim, MD^a

Abstract

It is difficult to characterize the nodular lesions in cirrhotic liver if typical enhancement pattern is not present on dynamic contrast-enhanced imagings. Although the signal intensity of the hepatobiliary phase in gadoxetic acid-enhanced magnetic resonance imaging (MRI) is helpful for characterization of the lesions, some dysplastic nodules may also exhibit low signal intensity in the hepatobiliary phase. We aimed to assess the usefulness of gadoxetic acid (Gd-EOB-DTPA)-enhanced MRI including diffusion-weighted imaging (DWI) for differentiation between atypical small hepatocellular carcinomas (HCCs) and dysplastic nodules showing low signal intensity (SI) in the hepatobiliary phase, and to evaluate the MRI findings in determining the histological grade of atypical HCCs in patients with cirrhosis.

A total of 43 cirrhotic patients with a small (≤ 3 cm) liver nodule ($n=25$, HCC; $n=18$, dysplastic nodule) who underwent Gd-EOB-DTPA-enhanced MRI and pathologic confirmation were retrospectively reviewed. Atypical HCC was defined as not showing arterial hyperenhancement and delayed washout on dynamic MRI.

High SI on both T2WI and DWI (sensitivity 80.0%, specificity 100%, positive predictive value 100%, negative predictive value 78.3%) was the most specific feature to differentiate atypical HCCs from dysplastic nodules. High SI on both T2WI and DWI (100% vs 61.5%, $P=.039$) or low SI on pre-enhanced T1WI (83.3% vs 30.8%, $P=.021$) was more frequent observed in Edmonson grade II–III HCCs compared with those in grade I HCCs.

The combination of DWI and T2WI is most useful for the differentiation of atypical small HCCs from dysplastic nodules showing low SI in the hepatobiliary phase. Combination of DWI and T2WI or pre-enhanced T1WI seems to be useful for predicting the histological grade of atypical HCCs.

Abbreviations: AASLD = American Association for the Study of Liver Disease, AFP = alpha-fetoprotein, AUC = area under the curve, CT = computed tomography, DWI = diffusion-weighted imaging, Gd-EOB-DTPA = gadolinium-ethoxybenzyl-diethylenetriamine pentaacetic acid, HCC = Hepatocellular carcinoma, MRI = magnetic resonance imaging, NPV = negative predictive value, OATP = organic anionic transporting polypeptides, PIVKA-II = protein induced by vitamin K absence or antagonist-II, PPV = positive predictive value, ROC = receiver operating characteristic, SI = signal intensity, T1WI = T1-weighted imaging, T2WI = T2-weighted imaging, TE = echo time, TR = repetition time.

Keywords: diffusion-weighted magnetic resonance imaging, dysplastic nodule, hepatocellular carcinoma, histological grade, T2-weighted imaging

Editor: Muhammed Mubarak.

The authors have no conflicts of interest to declare.

^a Department of Internal medicine, ^b Department of Radiology, ^c Department of Pathology, Gachon University Gil Medical Center, Incheon, Republic of Korea.

* Correspondence: Yun Soo Kim, Division of Gastroenterology and hepatology, Department of Internal Medicine, Gachon University Gil Medical Center, 21, Namdong-daero 774 beon-gil, Namdong-gu, Incheon 21565, Republic of Korea (e-mail: kimys@gilhospital.com).

Copyright © 2017 the Author(s). Published by Wolters Kluwer Health, Inc. This is an open access article distributed under the terms of the Creative Commons Attribution-Non Commercial License 4.0 (CCBY-NC), where it is permissible to download, share, remix, transform, and buildup the work provided it is properly cited. The work cannot be used commercially without permission from the journal.

Medicine (2017) 96:29(e7278)

Received: 9 March 2017 / Received in final form: 1 June 2017 / Accepted: 5 June 2017

<http://dx.doi.org/10.1097/MD.0000000000007278>

1. Introduction

Hepatocellular carcinoma (HCC) is one of the most common cancers worldwide and the third most common cause of cancer-related death.^[1,2] There is a growing incidence of HCC worldwide. Most patients with HCC have liver cirrhosis, which develops following long periods of chronic liver disease caused by hepatitis viruses, alcohol, non-alcoholic fatty liver disease, and inherited metabolic diseases, such as hemochromatosis or alpha-1-antitrypsin deficiency.^[3] The prognosis for patients with HCC is poor because the majority of patients that present with HCC are already at an intermediate or advanced stage and are not suitable for curative treatment.^[4] To increase the chance of curative treatment and to improve survival, the detection of HCC at early stage is an important therapeutic strategy.

Typical imaging features of HCC, such as arterial enhancement and delayed wash-out, are highly specific for the diagnosis of HCC.^[5] On the other hand, some HCCs, particularly those smaller than 2 to 3 cm in diameter and well-differentiated HCCs lacking a typical enhancement pattern, are challenging to diagnose; at this early stage, arterial tumor vessels have not sufficiently developed.^[6,7] Confirmation by liver biopsy is required to diagnose hepatic nodules that do not demonstrate a typical enhancement pattern.^[8] However, percutaneous biopsy is invasive and may not always be possible due to the location of lesion, the presence of ascites, or a bleeding tendency in patients with cirrhosis. Therefore, additional non-invasive imaging techniques are required for the differentiation of indeterminate hepatic nodules.

Gadolinium ethoxybenzyl diethylenetriamine pentaacetic acid (Gd-EOB-DTPA; gadoteric acid) is a liver-specific contrast agent taken up specifically by hepatocytes. Gd-EOB-DTPA is widely used to improve the detectability of focal liver lesions and the characterization of liver tumors on magnetic resonance imaging (MRI).^[9] Several studies have shown that differentiation between well-differentiated HCCs and hepatic pseudolesions, such as regenerative nodules or arteriportal shunts, can be improved by using hepatobiliary phase images of Gd-EOB-DTPA-enhanced MRI.^[10,11] However, benign hepatocellular lesions, such as dysplastic nodules which can also be seen as low signal intensity (SI) on hepatobiliary phase images, are difficult to distinguish from HCCs.^[12] Recently, several studies have shown that detection of well-differentiated HCC with insufficient development of arterial vessels can be improved with alternative imaging modalities, such as diffusion-weighted imaging (DWI), computed tomography (CT) angiography, and contrast-enhanced ultrasound.^[13–17]

In addition, the histologic grade of HCC is an important prognostic factor of patient outcome.^[18] Therefore, it is also necessary to predict histological differentiation of atypical HCC via non-invasive methods.

This study was conducted to assess the usefulness of Gd-EOB-DTPA-enhanced MRI including DWI for differentiation between atypical small HCCs and dysplastic nodules showing low SI in the hepatobiliary phase, and to evaluate the MRI findings in determining the histological grade of atypical HCCs in patients with cirrhosis.

2. Patients and methods

2.1. Patients

We conducted a retrospective study of 90 patients with cirrhosis with a single liver nodule ≤ 3 cm in diameter showing low SI in the hepatobiliary phase of Gd-EOB-DTPA-enhanced MRI between December 2008 and December 2015. Gd-EOB-DTPA-enhanced MRI and DWI were performed, and pathologic evaluation was performed in all the patients. Atypical HCC was defined as not showing typical enhancement (arterial hyperenhancement and delayed washout) on dynamic MRI. Of these, 53 patients with liver nodule showing typical enhancement pattern on dynamic MRI were excluded. The atypical vascular pattern was observed in 43 nodules (arterial hypervascular nodule without delayed wash-out in 11 patients; arterial hypovascular nodule in 32 patients). Of the 43 nodules, 25 nodules were pathologically confirmed as HCCs and 18 nodules were confirmed as dysplastic nodules ($n = 12$, high-grade; $n = 6$, low-grade). Liver cirrhosis was diagnosed by liver biopsy, or according to radiologic findings

such as coarse hepatic echotexture with surface nodularity or the presence of features of portal hypertension (e.g., ascites, splenomegaly, and varices) noted on liver imaging.^[19,20]

Clinical and laboratory parameters, MRI findings, and final pathologic diagnoses were analyzed. The study protocol was approved by the Institutional Review Board (IRB) of Gachon University Gil Medical Center (IRB No. GAIRB2015–346).

2.2. Magnetic resonance imaging

Magnetic resonance images were obtained using a 3 T MRI system (Verio, Siemens Medical Solutions, Erlangen, Germany). The MRI protocol consisted of a breath-hold fat-saturated T2-weighted fast spin-echo or turbo spin-echo sequence, a breath-hold T1-weighted dual-echo (in-phase and opposed-phase) sequence, pre-contrast and three-dimensional fat-saturated T1-weighted dynamic contrast-enhanced sequences, and free-breathing DWI, using a single-shot echo-planar imaging sequence, and 20 minutes delayed hepatobiliary phase. For the contrast-enhanced dynamic MR images, Gd-EOB-DTPA (Primovist, Eovist; Bayer-Schering, Berlin, Germany) was administered at 0.025 mmol/kg of body weight at 2 mL/s. Arterial phase images were acquired 7 seconds after arrival of the contrast medium at the thoracic aorta, and portal venous, delayed, and hepatobiliary phase images were subsequently acquired 60 seconds, 180 seconds, and 20 minutes, respectively. Diffusion-weighted imaging with simultaneous respiratory triggering was performed during the period prior to the 20 minutes delayed imaging. For each patient, the repetition time was matched to the length of the respiratory cycle; every patient had b -values of 0, 400, and 1000 s/mm². The apparent diffusion coefficient (ADC) value of the HCC was measured on an ADC map, and the slice's location was identical to that of the selected image on the DW images and hepatobiliary phase images. The ADC value was automatically calculated by a computer program included in the GE workstation software. The MR images were retrospectively analyzed by 2 radiologists who were unaware of the pathologic results.

2.3. Histology of liver nodules

Ultrasound-guided percutaneous biopsy ($n = 36$) or surgical resection ($n = 7$) was performed for histological evaluation. Tru-cut biopsy needles (ACE-CUT biopsy needle, TSK) were used for sonography-guided percutaneous biopsy and at least 2 biopsies were obtained from each patient. The diagnosis of nodular hepatocellular lesions was based on International Working Party criteria.^[21] The diagnostic features of small well-differentiated HCC were as follows: increased cell density, more than twice that of surrounding liver, with increase nucleus/cytoplasm ratio; irregular thin trabecular pattern of growth; pseudo-glandular structures; fatty change; unpaired arteries; and intra-tumoral portal tracts.^[22] The histological grade of tumor differentiation was determined according to the modified Edmondson–Steiner grading system.^[23]

Dysplastic nodules were defined as the presence of regions of hepatocytes at least 1 mm in diameter with dysplasia, but no definite histological signs of malignancy. Dysplastic nodules were classified as low- or high-grade dysplastic nodules based on the cytological and architectural atypia. In order to eliminate interobserver variation in diagnosis of the liver nodules, all histology slides were reviewed by a single experienced hepatopathologist. Markers of HCC such as glypican-3 and glutamine synthetase were used for the differentiation between early HCCs

and dysplastic nodules. When more than 1 histological grade is observed in the tumor, the major grade was recorded for the analysis.

2.4. Statistical analysis

Quantitative data were expressed as medians (ranges). The Mann–Whitney *U* test was used to compare means, and the chi-square test or Fisher exact test was used to compare differences in MRI findings between atypical small hepatocellular carcinomas (HCCs) and dysplastic nodules. The sensitivity, specificity, positive predictive value (PPV), negative predictive value (NPV), and the area under the receiver operating characteristic (ROC) curve (AUC) were used to determine the diagnostic usefulness of the MRI findings in differentiating between dysplastic nodules and HCC. Recurrence-free survival was calculated by the Kaplan–Meier method, and differences in survival between the groups were compared using the log-rank test. Statistical significance was accepted for $P < .05$. Statistical analyses were performed using the SPSS version 12.0 software package (SPSS Inc, Chicago, IL).

3. Results

3.1. Baseline characteristics

The mean age of the 43 patients was 58.8 ± 10.8 years, and 31 patients (72.1%) were men. All patients had been diagnosed with cirrhosis. The cause of liver cirrhosis was hepatitis B virus in 29 patients (67.4%), hepatitis C virus in 8 patients (18.6%), and alcohol in 6 patients (14.0%). Tumor nodules were categorized into 3 groups: Edmondson grade I HCC ($n=13$), Edmondson grade II–III HCC (grade II, $n=5$; grade III, $n=7$), and dysplastic nodule (high grade, $n=12$; low grade, $n=6$). There were no Edmondson grade IV tumors in the present study. Median tumor sizes in these 3 groups were 1.8 cm (1.0–3.0 cm), 2.0 cm (1.0–2.7 cm) and 1.8 cm (1.0–3.0 cm), respectively. Tumor size and tumor markers such as alpha-fetoprotein (AFP) and protein induced by vitamin K absence or antagonist-II (PIVKA-II) were not statistically different among the 3 groups (Table 1).

3.2. Magnetic resonance imaging features in the differentiation of atypical HCCs and dysplastic nodules

Low SI on pre-enhanced T1-weighted imaging (T1WI) was observed in 56% (14/25) of the atypical HCCs. High SI on pre-enhanced T1WI was observed in 39% (7/18) of dysplastic nodules ($n=7$, high grade; $n=0$, low grade). High SI on T2WI

was observed in 88% (22/25) of atypical HCCs. Low SI or iso SI on T2WI was observed in 78% (14/18) of dysplastic nodules. High SI on DWI was observed in 80% (20/25) of atypical HCCs. Iso or low SI on DWI was observed in 94.4% (17/18) of dysplastic nodules. High SI on both T2WI and DWI was observed in 80% (20/25) of atypical HCCs.

Compared with the SI values on MRI in patients with dysplastic nodules, low SI on pre-enhanced T1WI ($P=.012$), high SI on T2WI ($P < .001$), and high SI ($P < .001$) on DWI and high SI on both T2WI and DWI ($P < .001$) were more frequently observed in patients with atypical HCCs.

In differentiating between atypical HCCs and dysplastic nodules, high SI on DWI (sensitivity 80.0%, specificity 94.4%, PPV 95.2%, NPV 77.3%) yielded the best results among MRI sequences. The combination of high SI on T2WI and DWI (sensitivity 80.0%, specificity 100%, PPV 100%, NPV 78.3%) demonstrated the highest specificity in differentiating between atypical HCCs and dysplastic nodules. However, delayed wash-out on dynamic T1WI was not appropriate method for differentiation of atypical HCCs and dysplastic nodules. The specific values of ROC curve in differentiating between atypical HCCs and dysplastic nodules are summarized in Table 2.

In addition, the combination of high SI on T2WI and DWI (sensitivity 61.5%, specificity 100%, PPV 100%, NPV 70.6%) demonstrated the highest specificity in differentiating between atypical Edmondson grade I HCCs and high-grade dysplastic nodules. On the other hand, pre-enhanced T1WI represented a sensitive method for the differentiation of atypical Edmondson grade I HCCs and high-grade dysplastic nodules. The specific values of ROC curve in differentiating between atypical Edmondson grade I HCCs and high-grade dysplastic nodules are summarized in Table 3.

High SI on both DWI and T2WI was the most diagnostic valuable method for differentiating between atypical HCCs and dysplastic nodules as well as for differentiating between atypical Edmondson grade I HCCs and high-grade dysplastic nodules based on ROC curves (Fig. 1).

3.3. Differences of MRI features between Edmondson grade II–III HCCs and grade I HCCs/dysplastic nodules

Low SI on pre-enhanced T1WI was observed more frequently in Edmondson grade II–III HCCs (10/12, 83.3%) than in Edmondson grade I HCCs (4/13, 30.8%) ($P=.021$). High SI on DWI was observed more frequently in Edmondson grade II–III HCCs (12/12, 100%) than in Edmondson grade I HCCs (8/13, 61.5%) ($P=.039$). High SI on both T2WI and DWI was observed more frequently in Edmondson grade II–III HCCs (12/12, 100%)

Table 1

Baseline characteristics of the patients.

	Edmondson grade I HCC (n=13)	Edmondson grade II–III HCC (n=12)	Dysplastic nodule (n=18)	P
Age (y, median [range])	63 (48–82)	44 (31–56)	63 (43–81)	.022
Sex (male) (n, %)	11 (84.6%)	10 (83.3%)	10 (55.6%)	.181
Etiology				.510
HBV (n, %)	8 (61.5%)	10 (83.3%)	11 (61.1%)	
HCV (n, %)	2 (15.4%)	2 (16.7%)	4 (22.2%)	
Alcohol (n, %)	3 (23.1%)	0 (0%)	3 (16.7%)	
Tumor size (cm, median [range])	1.8 (1.0–3.0)	2.0 (1.0–2.7)	1.8 (1.0–3.0)	.769
AFP (ng/mL, median [range])	9.2 (2.3–21.3)	4.1 (1.3–189.6)	10.5 (4.6–76.5)	.843
PIVKA-II (mAu/mL, median [range])	26 (13–173)	26 (15–1116)	25 (16–220)	.827

AFP = alpha-fetoprotein, HBV = hepatitis B virus, HCC = hepatocellular carcinoma, HCV = hepatitis C virus; MRI = magnetic resonance imaging, PIVKA-II = protein induced by vitamin K absence or antagonist-II.

Table 2

Sensitivity and specificity of Gd-EOB-DTPA-enhanced and diffusion-weighted magnetic resonance imaging findings for the differentiation of atypical small (≤ 3 cm) hepatocellular carcinomas and dysplastic nodules.

	Sensitivity (%)	Specificity (%)	PPV (%)	NPV (%)	AUC (95% CI)	P
Iso or low SI on pre-enhanced T1WI	96.0% (24/25)	38.9% (7/18)	68.6% (24/35)	87.5% (7/8)	0.674 (0.503–0.846)	.053
Delayed wash-out on dynamic T1WI	64.0% (16/25)	50.0% (9/18)	64.0% (16/25)	50.0% (9/18)	0.570 (0.394–0.746)	.438
High SI on T2WI	84.6% (22/25)	77.8% (14/18)	84.6% (22/26)	82.4% (14/17)	0.829 (0.693–0.965)	<.001
High SI on DWI	80.0% (20/25)	94.4% (17/18)	95.2% (20/21)	77.3% (17/22)	0.872 (0.759–0.986)	<.001
High SI on T2WI plus high SI on DWI	80.0% (20/25)	100% (18/18)	100% (20/20)	78.3% (18/23)	0.900 (0.802–0.998)	<.001
Iso or low SI on pre-enhanced T1WI plus high SI on T2WI	88.0% (22/25)	83.3% (15/18)	88.0% (22/25)	83.3% (15/18)	0.857 (0.731–0.982)	<.001
Iso or low SI on pre-enhanced T1WI plus high SI on DWI	80.0% (20/25)	94.4% (17/18)	95.2% (20/21)	77.3% (17/22)	0.872 (0.759–0.986)	<.001

AUC = area under the curve, CI = confidence interval, DWI = diffusion-weighted imaging, Gd-EOB-DTPA = gadolinium-ethoxybenzyl-diethylenetriamine pentaacetic acid, NPV = negative predictive value, PPV = positive predictive value, SI = signal intensity, T1WI = T1-weighted imaging, T2WI = T2-weighted imaging.

than in Edmonson grade I HCCs (8/13, 61.5%) ($P = .039$). However, median ADC values were not significantly different between Edmonson grade I HCCs ($0.84 \times 10^{-3} \text{ mm}^2/\text{s}$, range 0.80–1.03) and Edmondson grade II–III HCCs ($0.91 \times 10^{-3} \text{ mm}^2/\text{s}$, range 0.74–1.24) ($P = .524$) (data not shown). Of the 25 patients with pathologically diagnosed HCC, 8 patients underwent surgery, 10 underwent radiofrequency ablation (RFA), 4 underwent percutaneous ethanol injection (PEI), and 1 underwent transarterial chemoembolization (TACE). The remaining 2 patients were lost to follow-up. During a median follow-up period of 23 months (range, 1–50 months) after treatment, the recurrence was observed in 37.5% (3/8) patients who underwent surgery, 50.0% (5/10) patients who underwent RFA, 25.0% (1/4) patients who underwent PEI, and 100% (1/1) patients who underwent TACE. There was no statistical difference in recurrence according to treatment method ($P = .674$). Recurrence-free survival in the group showing high SI on both T2WI and DWI was significantly lower than that in the group not showing high SI on both T2WI and DWI according to analysis using the Kaplan–Meier method with the log-rank test ($P = .004$) (Fig. 2).

High SI on pre-enhanced T1WI was observed more frequently in high-grade dysplastic nodules (7/12, 58.3%) or Edmondson grade I HCCs (2/13, 15.4%) than in Edmondson grade II–III HCCs (0/12, 0%). Low SI on pre-enhanced T1WI was more commonly observed in Edmondson grade II–III HCCs than Edmondson grade I HCCs or dysplastic nodules (Fig. 3).

4. Discussion

The 2005 guidelines from the European Association for the Study of the Liver and the American Association for the Study of Liver Diseases (AASLD) suggested that HCC could be diagnosed

without a biopsy in nodules > 2 cm when a typical enhancement pattern was observed on 1 dynamic imaging modality.^[24] The updated AASLD guidelines propose that 1 imaging technique (CT or MRI) showing a typical enhancement pattern is sufficient for the diagnosis of HCC in 1 to 2 cm nodules in patients with cirrhosis of any etiology or patients with chronic hepatitis B who may not have fully developed cirrhosis or have regressed cirrhosis.^[8]

However, in our study, the typical enhancement pattern was not observed in 50.0% of Edmondson grade I and 26.6% of Edmondson grade II–III HCCs < 3 cm in diameter. Several studies have also demonstrated that 27% to 34% of small HCCs show atypical enhancement features, such as hypovascular patterns.^[25–28]

In functioning hepatocytes, organic anionic transporting polypeptide (OATP)-8 is responsible for uptake of 2 gadolinium-based contrast agents: Gd-EOB-DTPA and gadobenate dimeglumine. Nodules with low, or no, organic anionic transporting polypeptides (OATP) expression do not take up hepatobiliary agents and appear as hypointense areas during the hepatobiliary phase.^[29] Recent reports suggest that most HCCs and some high-grade dysplastic nodules demonstrate hypointensity during the hepatobiliary phase due to under-expression of OATP.^[30] Furthermore, it has been reported that most cirrhotic nodules appear as isointense or hyperintense areas due to the preserved expression of OATP.^[13] In cases of liver nodules showing low SI in the hepatobiliary phase with atypical enhancement patterns, the differential diagnosis between HCCs and dysplastic nodules may be very challenging.

Diffusion-weighted MRI has recently been proposed as an additional unenhanced MRI sequence for the diagnosis of HCC.^[31] Xu et al^[32] reported a higher sensitivity for DWI with a b -value of 500 s/mm^2 , compared with conventional MRI for the detection of HCC in cirrhotic liver (98% for DWI vs 83–85% for conventional MRI). On the other hand, Rhee et al^[12] reported

Table 3

Sensitivity and specificity of Gd-EOB-DTPA-enhanced and diffusion-weighted magnetic resonance imaging findings for the differentiation of atypical Edmondson grade I hepatocellular carcinomas and high-grade dysplastic nodules.

	Sensitivity (%)	Specificity (%)	PPV (%)	NPV (%)	AUC (95% CI)	P
Iso or low SI on pre-enhanced T1WI	92.3% (12/13)	58.3% (7/12)	70.6% (12/17)	87.5% (7/8)	0.753 (0.552–0.945)	.032
Delayed wash-out on dynamic T1WI	69.2% (9/13)	50.0% (6/12)	60.0% (9/15)	60.0% (6/10)	0.596 (0.369–0.823)	.415
High SI on T2WI	76.9% (10/13)	75.0% (9/12)	76.9% (10/13)	75.0% (9/12)	0.760 (0.562–0.957)	.028
High SI on DWI	61.5% (8/13)	91.7% (11/12)	88.9% (8/9)	68.8% (11/16)	0.766 (0.572–0.960)	.024
High SI on T2WI plus high SI on DWI	61.5% (8/13)	100% (12/12)	100% (8/8)	70.6% (12/17)	0.808 (0.628–0.982)	.009
Iso or low SI on pre-enhanced T1WI plus high SI on T2WI	76.9% (10/13)	83.3% (10/12)	83.3% (10/12)	76.9% (10/13)	0.801 (0.617–0.985)	.011
Iso or low SI on pre-enhanced T1WI plus high SI on DWI	61.5% (8/13)	91.7% (11/12)	88.9% (8/9)	68.8% (11/16)	0.766 (0.572–0.960)	.024

AUC = area under the curve, CI = confidence interval, DWI = diffusion-weighted imaging, Gd-EOB-DTPA = gadolinium-ethoxybenzyl-diethylenetriamine pentaacetic acid, NPV = negative predictive value, PPV = positive predictive value, SI = signal intensity, T1WI = T1-weighted imaging, T2WI = T2-weighted imaging.

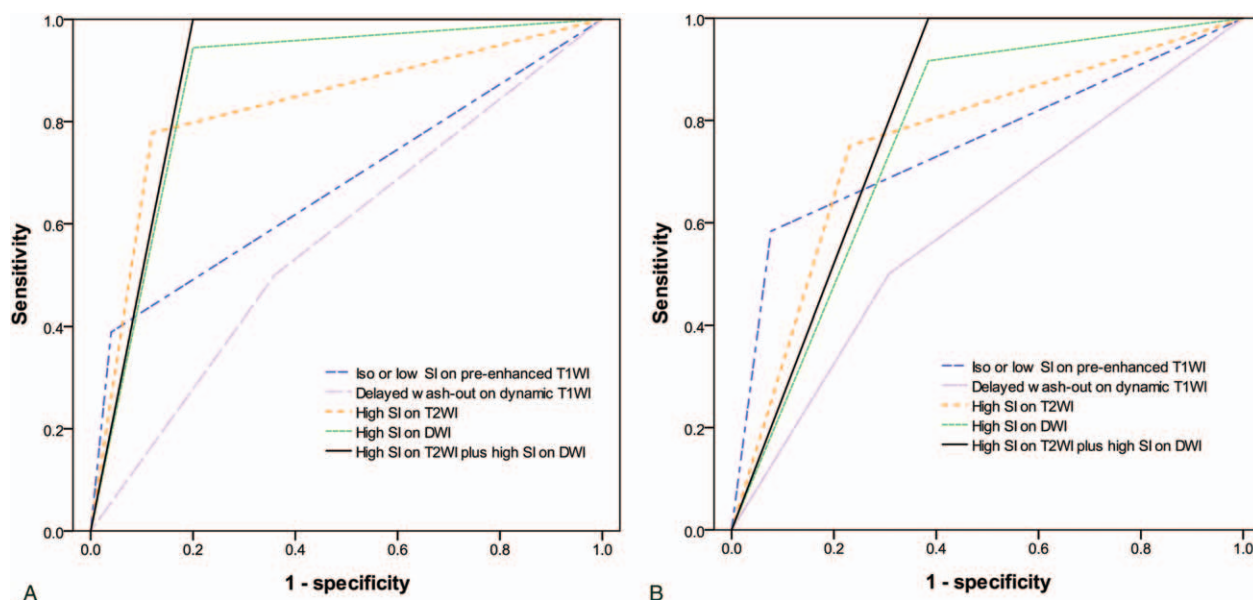


Figure 1. ROC curves of Gd-EOB-DTPA-enhanced and diffusion-weighted MRI findings (A) for the differentiation of atypical small (≤ 3 cm) HCCs from dysplastic nodules, and (B) for the differentiation of Edmonson grade I HCCs from high-grade dysplastic nodules. DWI=diffusion-weighted imaging, Gd-EOB-DTPA=gadolinium-ethoxybenzyl-diethylenetriamine pentaacetic acid, HCC=hepatocellular carcinoma, MRI=magnetic resonance imaging, ROC=receiver operating characteristic, SI=signal intensity, T1WI=T1-weighted imaging, T2WI=T2-weighted imaging.

that the sensitivity of hyperintensity on DWI with a high b -value ($b=800$ s/mm²) in the diagnosis of early HCC was very low (13.8%). Clinically, several DW images can be obtained by altering the strength and magnitude of the applied gradients; these images are referred to as DW images at a particular b -value.^[31] Low b -values could lead to overestimation of benign lesions and high b -values could lead to lower sensitivity rates in

the detection of well-differentiated HCCs.^[33] In our study, high SI on DWI with a b -value of 400 s/mm² (sensitivity 84.0%, specificity 94.4%, PPV 95.5%, NPV 81.0%) was the best single sequence capable of differentiating between atypical HCCs and dysplastic nodules.

Several studies have evaluated the diagnostic value of T2WI in the characterization of HCCs in cirrhotic and non-cirrhotic liver, with varying results.^[34,35] Chou et al^[36] demonstrated that hyperintensity on T2WI was helpful in differentiating between dysplastic nodules and well-differentiated HCCs. On the other hand, Hussain et al^[37] concluded that T2WI did not provide any additional diagnostic value in the detection and characterization of focal lesions in cirrhotic liver, because scar tissue in cirrhotic liver could occasionally mimic HCC on T2WI.^[38,39] In our study of atypical HCCs and dysplastic nodules, the sensitivity and specificity of high SI on T2WI in the diagnosis of HCC were 84.6% and 77.8%, respectively. These results may have been influenced by the design of this study which excluded other influencing factors such as benign mature fibrous tissue. Consequently, the combination of T2WI and DWI with a b -value of 400 s/mm² was most specific feature in distinguishing between atypical HCCs and dysplastic nodules, compared with DWI alone.

Recently, many efforts have focused on the non-invasive evaluation of the differentiation grade of HCC using MRI findings because the histological grade of HCC is a significant prognostic factor after treatment. Okamoto et al^[40] reported a relationship between the histological grade of HCC and wash-out on dynamic contrast-enhanced MRI. Muhi et al^[41] suggested that DWI may be closely related to the histology of the hepatocellular lesions. Chou et al^[36] showed that loss of hyperintensity on T1WI and the detection of arterial enhancement may indicate further progression of the histological grade. In addition, Guo et al^[42] demonstrated that the ADC value based on DWI is useful in determining the histological grade of HCC. In our study, low SI on pre-enhanced T1WI or high SI on both T2WI and DWI were

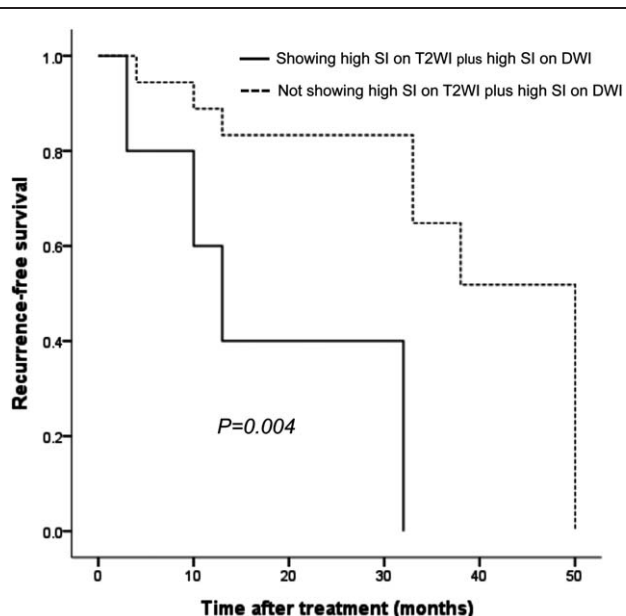


Figure 2. Comparison of tumor recurrence-free survival after treatment between tumor showing high SI on T2WI plus high SI on DWI and tumor not showing high SI on T2WI plus high SI on DWI in cirrhotic patients with a small (≤ 3 cm) HCC by Kaplan–Meier survival analysis. DWI=diffusion-weighted imaging, HCC=hepatocellular carcinoma, SI=signal intensity, T2WI=T2-weighted imaging.

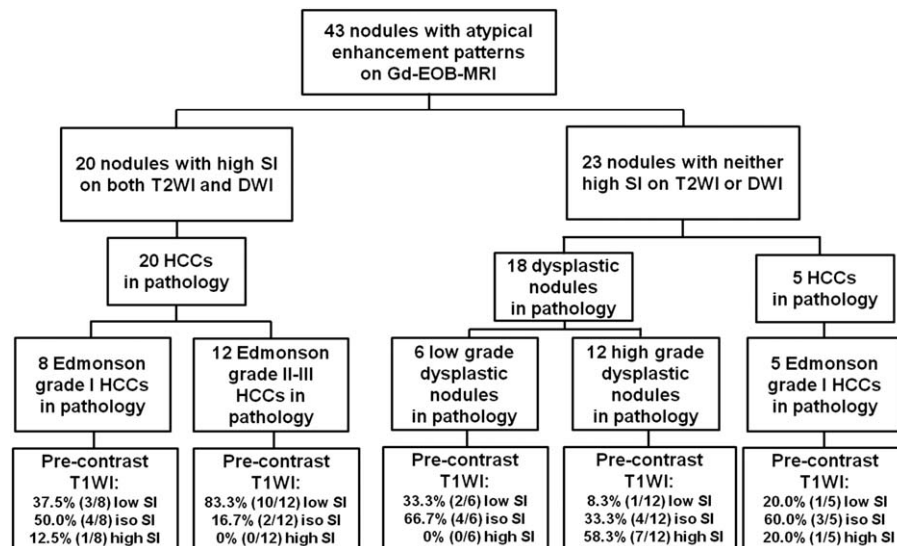


Figure 3. Usefulness of combination of DWI and T2WI and pre-enhanced T1WI in differentiating between atypical small (≤ 3 cm) hepatocellular carcinomas and dysplastic nodules, and in determining the histological grade of atypical HCCs in patients with cirrhosis. DWI=diffusion-weighted imaging, HCC=hepatocellular carcinoma, SI=signal intensity, T1WI=T1-weighted imaging, T2WI=T2-weighted imaging.

significantly different between Edmondson grade II–III HCCs and Edmondson grade I HCCs. Although there was a limit to the different treatment methods, there was a difference in recurrence-free survival after treatment according to whether high SI on both T2WI and DWI was seen in patients with atypical HCC. However, the wash-out on dynamic contrast-enhanced MRI and the ADC value based on DWI were not significantly different between Edmondson grade II–III HCCs and Edmondson grade I HCCs.

Our study has several limitations. First, many percutaneous biopsies were performed to determine the histopathological diagnoses and this technique is prone to sampling errors, particularly in small liver nodules. In order to minimize this limitation, we obtained 3 samples from each nodule using a 18-gauge needle. Second, all histology slides were reviewed by a single hepatopathologist in our study. If reviewed by more than 1 pathologist, the accuracy of diagnosis would be improved. However, the single pathologist has more than 20 years of experience in liver pathology, and markers of HCC such as glypican-3 and glutamine synthetase were used to improve diagnostic objectivity. Third, because of its retrospective design, there may have been selection bias in our study. However, a strength of this study is that all cases of atypical HCCs < 3 cm in patients with cirrhosis were confirmed pathologically with a relatively large scale.

In conclusion, the present study indicates that the combination of DWI and T2WI is a valuable technique for differentiating between small (≤ 3 cm) atypical HCCs and dysplastic nodules showing hypointensity in the hepatobiliary phase, as well as between atypical Edmondson grade I HCCs and high-grade dysplastic nodules in patients with cirrhosis. In addition, the study demonstrates the usefulness of pre-enhanced T1WI as well as the combination of DWI and T2WI in determining the histological differentiation grade of atypical HCCs. These results will help to diagnose small (≤ 3 cm) hepatic lesions, which are difficult to distinguish in cirrhosis, with atypical enhancement feature and hypointensity in hepatobiliary phase of gadoteric acid-enhanced MRI. Further large-scale studies would be warranted to assess the validity of diagnostic utility.

acid-enhanced MRI. Further large-scale studies would be warranted to assess the validity of diagnostic utility.

References

- [1] Jemal A, Ward E, Hao YP, et al. Trends in the leading causes of death in the United States, 1970–2002. *JAMA* 2005;294:1255–9.
- [2] Bosch FX, Ribes J, Diaz M, et al. Primary liver cancer: worldwide incidence and trends. *Gastroenterology* 2004;127:S5–16.
- [3] Di Bisceglie AM. Hepatitis B and hepatocellular carcinoma. *Hepatology* 2009;49:S56–60.
- [4] Mlynarsky L, Menachem Y, Shibolet O. Treatment of hepatocellular carcinoma: steps forward but still a long way to go. *World J Hepatol* 2015;7:566–74.
- [5] Forner A, Vilana R, Ayuso C, et al. Diagnosis of hepatic nodules 20 mm or smaller in cirrhosis: prospective validation of the noninvasive diagnostic criteria for hepatocellular carcinoma. *Hepatology* 2008;47:97–104.
- [6] Sugimachi K, Tanaka S, Terashi T, et al. The mechanisms of angiogenesis in hepatocellular carcinoma: angiogenic switch during tumor progression. *Surgery* 2002;131:S135–41.
- [7] Nicolau C, Catala V, Vilana R, et al. Evaluation of hepatocellular carcinoma using SonoVue, a second generation ultrasound contrast agent: correlation with cellular differentiation. *Eur Radiol* 2004;14:1092–9.
- [8] Bruix J, Sherman M. Management of hepatocellular carcinoma: an update. *Hepatology* 2011;53:1020–2.
- [9] Ichikawa T, Saito K, Yoshioka N, et al. Detection and characterization of focal liver lesions: a Japanese phase III, multicenter comparison between gadoteric acid disodium-enhanced magnetic resonance imaging and contrast-enhanced computed tomography predominantly in patients with hepatocellular carcinoma and chronic liver disease. *Invest Radiol* 2010;45:133–41.
- [10] Ahn SS, Kim MJ, Lim JS, et al. Added value of gadoteric acid-enhanced hepatobiliary phase MR imaging in the diagnosis of hepatocellular carcinoma. *Radiology* 2010;255:459–66.
- [11] Jeong WK, Kim YK, Song KD, et al. The MR imaging diagnosis of liver diseases using gadoteric acid: emphasis on hepatobiliary phase. *Clin Mol Hepatol* 2013;19:360–6.
- [12] Rhee H, Kim MJ, Park MS, et al. Differentiation of early hepatocellular carcinoma from benign hepatocellular nodules on gadoteric acid-enhanced MRI. *Br J Radiol* 2012;85:e837–44.
- [13] Kudo M. Multistep human hepatocarcinogenesis: correlation of imaging with pathology. *J Gastroenterol* 2009;44(Suppl):112–8.

- [14] Lee MH, Kim SH, Park MJ, et al. Gadoteric acid-enhanced hepatobiliary phase MRI and high-b-value diffusion-weighted imaging to distinguish well-differentiated hepatocellular carcinomas from benign nodules in patients with chronic liver disease. *AJR Am J Roentgenol* 2011;197:W868–75.
- [15] Kim T, Murakami T, Takahashi S, et al. Diffusion-weighted single-shot echoplanar MR imaging for liver disease. *AJR Am J Roentgenol* 1999; 173:393–8.
- [16] Nasu K, Kuroki Y, Tsukamoto T, et al. Diffusion-weighted imaging of surgically resected hepatocellular carcinoma: imaging characteristics and relationship among signal intensity, apparent diffusion coefficient, and histopathologic grade. *AJR Am J Roentgenol* 2009;193:438–44.
- [17] Shin SK, Kim YS, Choi SJ, et al. Contrast-enhanced ultrasound for the differentiation of small atypical hepatocellular carcinomas from dysplastic nodules in cirrhosis. *Dig Liver Dis* 2015;47:775–82.
- [18] Nathan H, Schulick RD, Choti MA, et al. Predictors of survival after resection of early hepatocellular carcinoma. *Ann Surg* 2009;249: 799–805.
- [19] Wong VW, Chan SL, Mo F, et al. Clinical scoring system to predict hepatocellular carcinoma in chronic hepatitis B carriers. *J Clin Oncol* 2010;28:1660–5.
- [20] Wong GL, Chan HL, Mak CW, et al. Entecavir treatment reduces hepatic events and deaths in chronic hepatitis B patients with liver cirrhosis. *Hepatology* 2013;58:1537–47.
- [21] Wanless IR. Terminology of nodular hepatocellular lesions. *Hepatology* 1995;22:983–93.
- [22] Kondo F. Histological features of early hepatocellular carcinomas and their developmental process: for daily practical clinical application: hepatocellular carcinoma. *Hepatol Int* 2009;3:283–93.
- [23] Edmondson HA, Steiner PE. Primary carcinoma of the liver: a study of 100 cases among 48,900 necropsies. *Cancer* 1954;7:462–503.
- [24] Bruix J, Sherman M. Management of hepatocellular carcinoma. *Hepatology* 2005;42:1208–36.
- [25] Heilmaier C, Lutz AM, Bolog N, et al. Focal liver lesions: detection and characterization at double-contrast liver MR Imaging with ferucarbotran and gadobutrol versus single-contrast liver MR imaging. *Radiology* 2009;253:724–33.
- [26] Kudo M. Imaging diagnosis of hepatocellular carcinoma and premalignant/borderline lesions. *Semin Liver Dis* 1999;19:297–309.
- [27] Hayashi M, Matsui O, Ueda K, et al. Progression to hypervascular hepatocellular carcinoma: correlation with intranodular blood supply evaluated with CT during intraarterial injection of contrast material. *Radiology* 2002;225:143–9.
- [28] Bolondi L, Gaiani S, Celli N, et al. Characterization of small nodules in cirrhosis by assessment of vascularity: the problem of hypovascular hepatocellular carcinoma. *Hepatology* 2005;42:27–34.
- [29] Choi JY, Lee JM, Sirlin CB. CT and MR imaging diagnosis and staging of hepatocellular carcinoma: part I. Development, growth, and spread: key pathologic and imaging aspects. *Radiology* 2014;272:635–54.
- [30] Sano K, Ichikawa T, Motosugi U, et al. Imaging study of early hepatocellular carcinoma: usefulness of gadoteric acid-enhanced MR imaging. *Radiology* 2011;261:834–44.
- [31] Parikh T, Drew SJ, Lee VS, et al. Focal liver lesion detection and characterization with diffusion-weighted MR imaging: comparison with standard breath-hold T2-weighted imaging. *Radiology* 2008;246: 812–22.
- [32] Xu PJ, Yan FH, Wang JH, et al. Added value of breathhold diffusion-weighted MRI in detection of small hepatocellular carcinoma lesions compared with dynamic contrast-enhanced MRI alone using receiver operating characteristic curve analysis. *J Magn Reson Imaging* 2009;29:341–9.
- [33] Vandecaveye V, De Keyzer F, Verslype C, et al. Diffusion-weighted MRI provides additional value to conventional dynamic contrast-enhanced MRI for detection of hepatocellular carcinoma. *Eur Radiol* 2009;19: 2456–66.
- [34] Pawluk RS, Tummala S, Brown JJ, et al. A retrospective analysis of the accuracy of T2-weighted images and dynamic gadolinium-enhanced sequences in the detection and characterization of focal hepatic lesions. *J Magn Reson Imaging* 1999;9:266–73.
- [35] Ward J, Baudouin CJ, Ridgway JP, et al. Magnetic resonance imaging in the detection of focal liver lesions: comparison of dynamic contrast-enhanced TurboFLASH and T2 weighted spin echo images. *Br J Radiol* 1995;68:463–70.
- [36] Chou CT, Chou JM, Chang TA, et al. Differentiation between dysplastic nodule and early-stage hepatocellular carcinoma: the utility of conventional MR imaging. *World J Gastroenterol* 2013;19: 7433–9.
- [37] Hussain HK, Syed I, Nghiem HV, et al. T2-weighted MR imaging in the assessment of cirrhotic liver. *Radiology* 2004;230:637–44.
- [38] Semelka RC, Chung JJ, Hussain SM, et al. Chronic hepatitis: correlation of early patchy and late linear enhancement patterns on gadolinium-enhanced MR images with histopathology initial experience. *J Magn Reson Imaging* 2001;13:385–91.
- [39] Ohtomo K, Baron RL, Dodd GD3rd, et al. Confluent hepatic fibrosis in advanced cirrhosis: evaluation with MR imaging. *Radiology* 1993;189: 871–4.
- [40] Okamoto D, Yoshimitsu K, Nishie A, et al. Enhancement pattern analysis of hypervascular hepatocellular carcinoma on dynamic MR imaging with histopathological correlation: validity of portal phase imaging for predicting tumor grade. *Eur J Radiol* 2012;81: 1116–21.
- [41] Muhi A, Ichikawa T, Motosugi U, et al. High-b-value diffusion-weighted MR imaging of hepatocellular lesions: estimation of grade of malignancy of hepatocellular carcinoma. *J Magn Reson Imaging* 2009;30:1005–11.
- [42] Guo W, Zhao S, Yang Y, et al. Histological grade of hepatocellular carcinoma predicted by quantitative diffusion-weighted imaging. *Int J Clin Exp Med* 2015;8:4164–9.